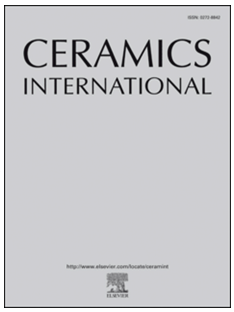
Journal Pre-proof



Silicon–calcium phosphate composite nanoparticles synthesized by laser ablation of a thermally oxidized porous silicon/hydroxyapatite composite

Filiz Karakuş Başak, Ersin Kayahan

PII: S0272-8842(21)01962-3

DOI: https://doi.org/10.1016/j.ceramint.2021.06.217

Reference: CERI 29257

To appear in: *Ceramics International*

Received Date: 3 May 2021

Revised Date: 18 June 2021

Accepted Date: 25 June 2021

Please cite this article as: Filiz.Karakuş. Başak, E. Kayahan, Silicon–calcium phosphate composite nanoparticles synthesized by laser ablation of a thermally oxidized porous silicon/hydroxyapatite composite, *Ceramics International* (2021), doi: https://doi.org/10.1016/j.ceramint.2021.06.217.

This is a PDF file of an article that has undergone enhancements after acceptance, such as the addition of a cover page and metadata, and formatting for readability, but it is not yet the definitive version of record. This version will undergo additional copyediting, typesetting and review before it is published in its final form, but we are providing this version to give early visibility of the article. Please note that, during the production process, errors may be discovered which could affect the content, and all legal disclaimers that apply to the journal pertain.

© 2021 Published by Elsevier Ltd.

Journal Pre-proof

Silicon-Calcium Phosphate Composite Nanoparticles Synthesized by Laser Ablation of a Thermally Oxidized Porous Silicon/Hydroxyapatite Composite

Filiz Karakuş Başak [1, 2, *] Ersin Kayahan [1, 3]

[1] Kocaeli University, Laser Technologies Research and Application Center (LATARUM), 41275, Yeniköy, Kocaeli, Turkey

[2] Kocaeli University, Biomedical Eng. Umuttepe, 41380, Kocaeli, Turkey

[3] Kocaeli University, Electro-Optics and Systems Eng. Umuttepe, 41380, Kocaeli, Turkey

***Corresponding Author**: filizkarakus@gmail.com*

Abstract

The TOPSi/HAP composite was obtained after heat treatment of thermally oxidized porous silicon (TOPSi) spin-coated with Hydroxyapatite (HAP) precursor solution. Silicon-Calcium Phosphate composite nanoparticles (SiCaPs) were synthesized in distilled water by laser ablation method using the TOPSi/HAP composite as the target material. According to Scanning Electron Microscopy (SEM), Fourier Transformed Infrared spectroscopy (FTIR), Energy-dispersive X-ray Spectroscopy (EDS), Dynamic Light Scattering (DLS) and Zeta Potential analyzes, SiCAPs are ultra-pure, spherical shaped nanoparticles with an average hydrodynamic diameter of 120 nm and a Zeta Potential of -20 mV for Ph 4,5. The proposed unique method enabled the SiCaPs synthesis. By changing some parameters of the synthesis conditions, SiCaPs of various properties can be designed for bone tissue engineering, wound healing, drug delivery, medical adhesives, and various biomedical applications.

Keywords: Hydroxyapatite, Calcium, Phosphate, Nanoparticles, Porous Silicon, Laser Ablation

1. Introduction

Silicon-calcium phosphate composite nanoparticles (SiCaPs) are therapeutic agents that can accelerate wound healing [1], and they can be tailored to the diseased area by loading various drugs [2,5]. They are important candidates for a variety of biomedical applications such as bone regeneration [3], hemorrhage control and medical adhesives [4]. The versatile utility of silicon-calcium phosphate composite nanoparticles makes them extremely attractive as biomaterials. Nanomaterials used in clinical applications must be of high purity, and it is essential that nanoparticles synthesis methods meet the requirements.

Most of the proposed methods for the synthesis of composite nanoparticles involve laborious processes, chemical impurities and harsh synthesis conditions. Compared to the traditional methods, nanoparticles synthesized by laser ablation method in liquid media have the desired shape and size, are nontoxic, and ultrapure since they do not contain chemical impurities [6]. During the nanosecond laser ablation process, a plasma plume which contains neutral atoms, ions, and electrons, is formed at the interface of the target material and the liquid medium. With the expansion and collapse of the plasma plume, these structures are released into the liquid medium in the form of nanoparticles [7]. The spongy structure of porous silicon has the ability to trap various molecules in their pores. Thus, it provides a great advantage in the preparation of numerous composite and hybrid materials [8-10]. Investigating the nanoparticle synthesis mechanism by short pulsed laser ablation in liquid medium, it was aimed to find out whether composite nanoparticles can be obtained when composite material is used as the target material.

This study which uses short pulsed laser source in distilled water, involves a unique method which enables a simple and pure process making possible the synthesis of SiCaPs for various biomedical applications such as bone tissue engineering, wound healing, drug delivery, medical adhesives. The TOPSi/HAP composite used as the target material as well as the synthesized SiCaPs were investigated by various analysis methods described in detail in the following sections. Ultra pure, spherical shaped SiCaPs with homogeneous size distribution were synthesized in a single step process by combining both the advantages of laser ablation method and the convenience provided by porous silicon in the production of composites. Composite nanoparticles of various structures can be synthesized by changing some of the parameters that affect the synthesis conditions of nanoparticles, such as laser parameters, liquid type, pore size of porous silicon, and the amount of HAP precursor solution.

2. Material and methods

2.1. Thermally Oxidized PSi (TOPSi) Production

The crystalline silicon (c-Si) wafers were cut into pieces to obtain a 1 cm^2 porous area. Silicon pieces were ultrasonically washed with acetone for 10 minutes. After rinsing with ethanol, it was dried on a fume hood at room temperature. PSi pieces were fabricated from n-type <111>, single crystal

(0.008–0.02 Ωcm) silicon wafers by electrochemical etching at 75 mA/cm² in a solution of (1:1) HF (38%): ethanol under 150 W lamp illumination for 45 minutes. PSi pieces were immersed in hydrogen peroxide (H_2O_2) (%28) solution for 30 minutes to create a uniform thin oxide layer. Finally, the PSi samples were thermally oxidized in a tube furnace at 950°C for one hour under anesthetic gas (N_2O) flow to form a $PSiO_2$ matrix, and then gradually cooled down under nitrogen (N_2) gas flow. The anesthetic gas and nitrogen gas flow were kept constant at 2500 sccm and 1000 sccm, respectively, with the aid of a flowmeter.

2.2. Synthesis of HAP Precursor Solution

HAP precursor solution was prepared using 4,682 g Calcium Nitrate Tetrahydrate ($Ca(NO_3)_2.4H_2O$, ≥%99, Merck), 2,320 g Dibutyl Phosphite ($[CH_3(CH_2)_3O]_2P(O)H$, ≥%96, Aldrich), 50 ml Ethyl alcohol (C_2H_6O, ≥%98, Merck). After all chemicals were added into the glass beaker, the magnetic stirrer was operated at a stirring speed of 200 rpm for 1 hour.

2.3. Preparation of TOPSi/HAP Composite

The HAP precursor solution in the syringe was dropped on the TOPSi one drop at every turn. Spin coating was carried out at a speed of 3000 rpm for 60 seconds. The process was repeated 10 times. The TOPSi/HAP composite was formed by heat treatment of TOPSi which was spin-coated with HAP precursor solution at 900°C for 1 hour.

2.4. SiCaPs Synthesis From TOPSi/HAP composite by Laser Ablation Method

The SiCaPs were synthesized using the laser ablation method by nanosecond pulsed laser in distilled water. The Nd:YAG laser parameters are 532 nm of wavelength, 6 ns of pulse-width, 10 Hz of frequency and 130 mJ of pulse energy. The target material (TOPSi/HAP) was placed in the middle of a pyrex beaker. The laser beam was focused on the TOPSi/HAP composite contained in a pyrex beaker filled with 5 ml of distilled water, using a plano convex (Newport model no: KPX103AR.33) lens (focal length 175 mm). The distance between the lens and the sample was set to 120 mm. The Pyrex beaker was positioned on a movable platform, and the platform was automatically moved continuously to achieve uniform irradiation of the entire TOPSi/HAP surface with the laser beam. A schematic representation of the synthesis steps of the SiCaPs is presented in Figure 1.

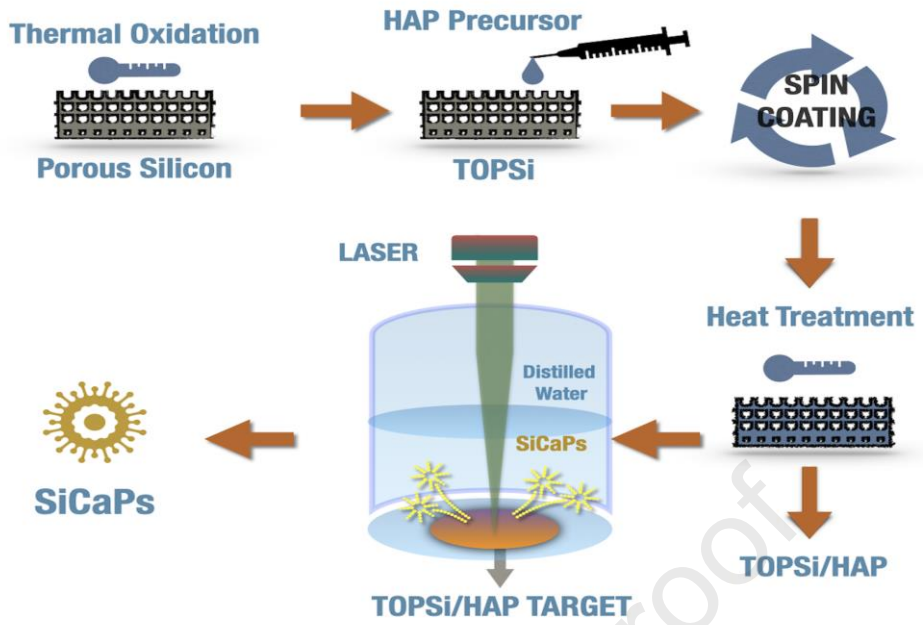


Fig. 1. The synthesis steps of SiCaPs

2.5. Characterization

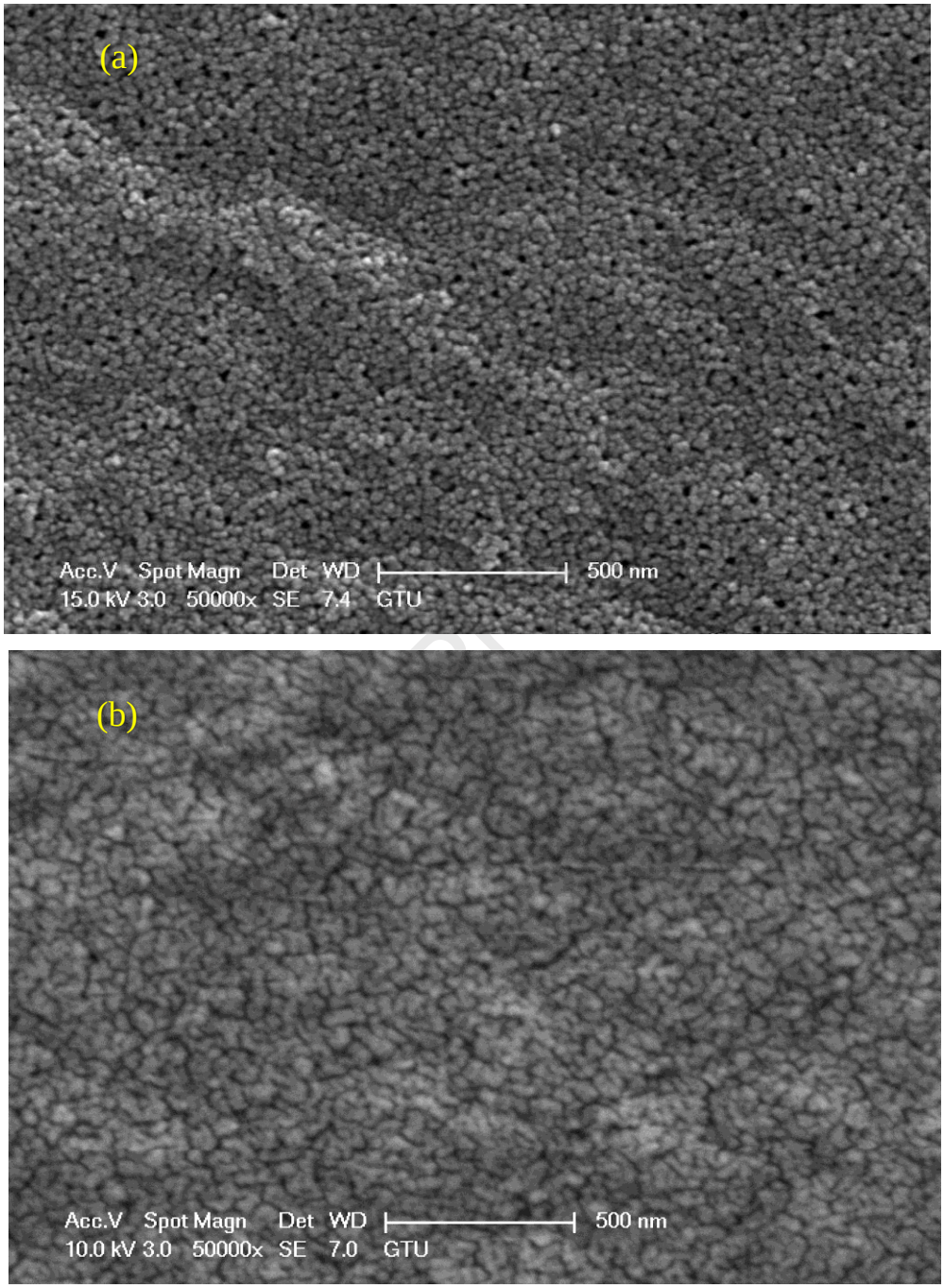
The properties of TOPSi, and of the TOPSi/HAP composite produced as target material were examined by FTIR, EDS and SEM. X-ray diffraction analysis (XRD) was used to determine the crystallographic structure of the TOPSi/HAP composite. The morphology and structure of SiCaPs were characterized by FTIR and EDS. The DLS and Zeta Potential analyses were performed to obtain the size distribution and surface zeta (ζ) potential of the SiCaPs, respectively. The synthesized SiCaPs were characterized by SEM to reveal their shapes and size distribution.

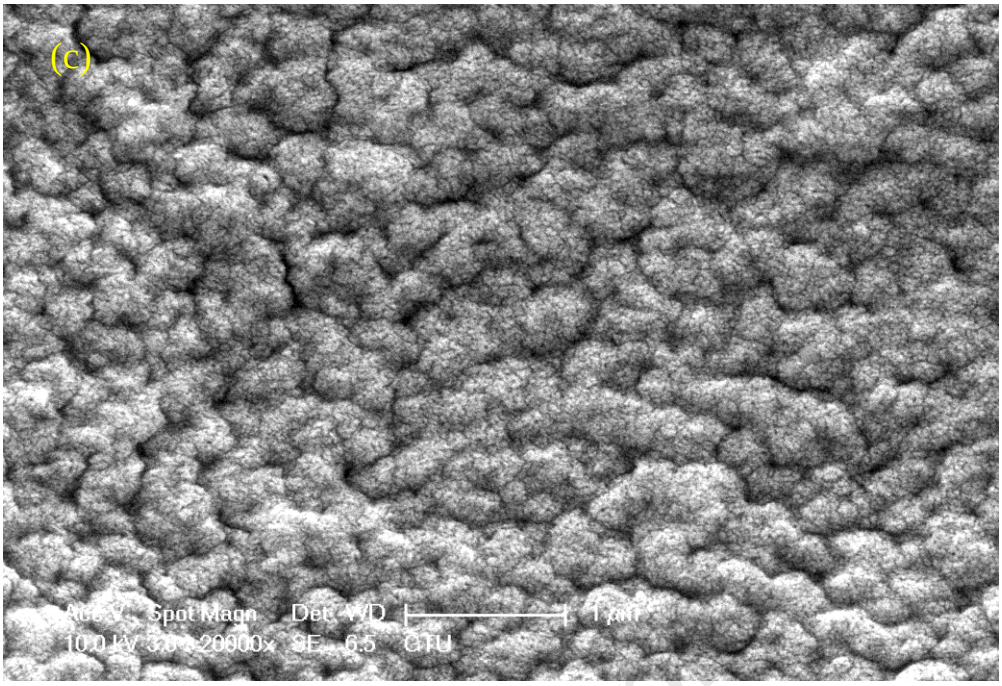
3. Result and Discussion

3.1. Characterization of TOPSi/HAP Composite

SEM image shown in Figure 2(a) revealed that PSi was formed, and SEM image shown in Figure 2(b) revealed that pore size and distribution changed as a result of thermal oxidation. In addition, it is clearly seen in Figure 2(c) that a new nanostructured TOPSi/HAP composite was formed as a result of the heat treatment applied after the HAP precursor solution was spin coated on TOPSi and absorbed into the pores. Both the particles and pores of the new nanostructure showed a highly homogeneous distribution. Fig. 2(d) shows the PL behavior of PSi and TOPSi under the 254 nm UV

lamp excitations. From the figure, it can be seen that the PL intensity dramatically decreased after the thermal oxidation.





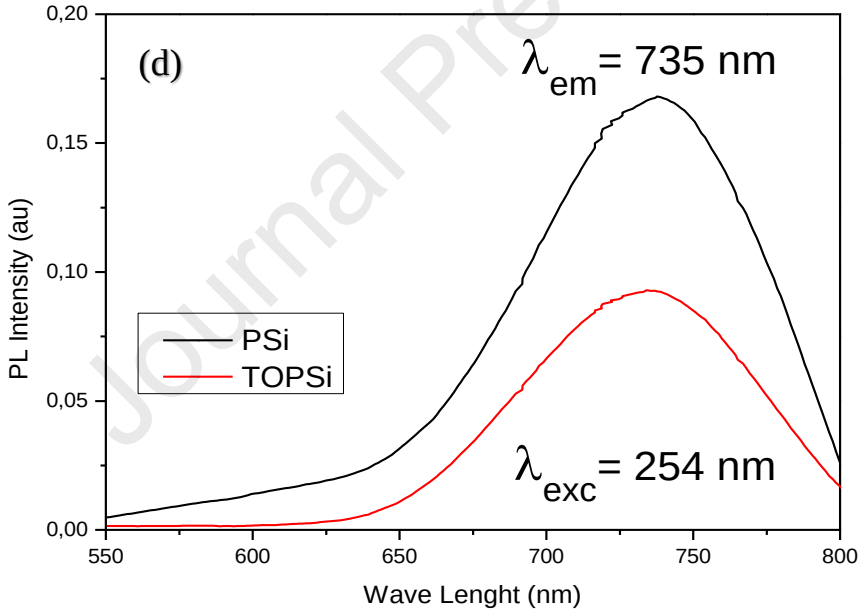


Fig. 2. SEM images **(a)** of PSi, **(b)** TOPSi, **(c)** TOPSi/HAP composite. PL spectra (d) of PSi and TOPSi

FTIR spectroscopy ranging from 600-4000 cm^{-1} was used to investigate the bond vibration modes of samples as shown in Figure 3. TOPSi exhibited absorption peaks at 1040 and 800 cm^{-1} indicating the presence of Si-O-Si stretching's. Absorption peaks were observed at 1090, 1030 cm^{-1}, indicating the presence of vibrational modes of $(PO_4)^{3-}$ after the formation of the TOPSi/HAP composite. The band attributed to the formation of the CaP phase increased and overlapped with the Si-O-Si stretching

modes at 800 cm^{-1}. The peak at 603 cm^{-1}, attributed to the formation of the CaP phase in the TOPSi/HAP composite, appeared sharply. Our FTIR results are consistent with both the data previously reported by Prokopowicz et al. [11] and cards created as a result of FTIR studies previously performed on porous silicon [12].

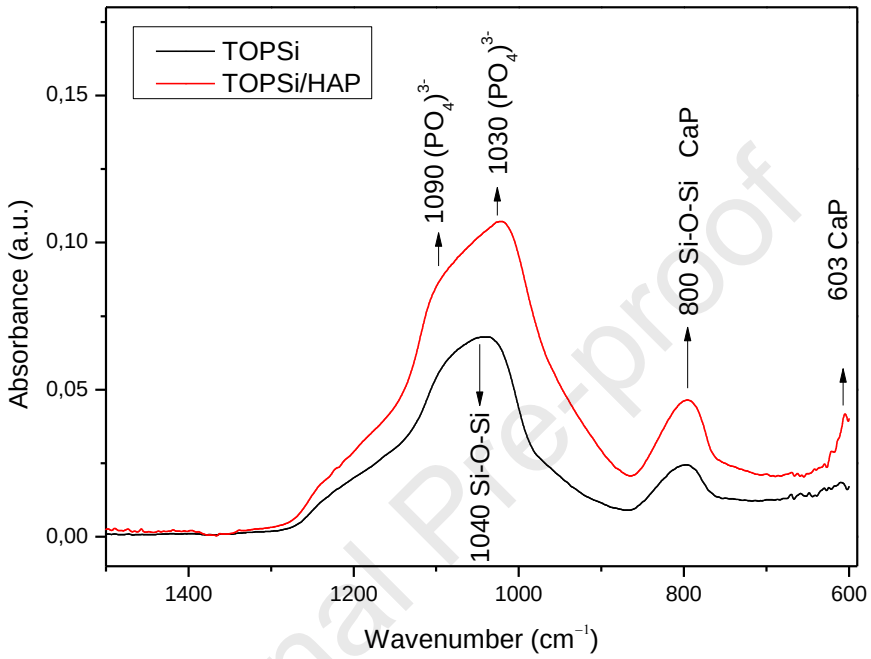


Fig. 3. FTIR spectra of TOPSi, and TOPSi/HAP composite

The results of the EDS analysis shown in Figure 4 were evaluated to further examine the TOPSi/HAP composite. After the TOPSi was spin-coated with the HAP precursor solution and finally heat treated, Ca and P peaks appeared, with the ratios shown in the table attached to the EDS plot.

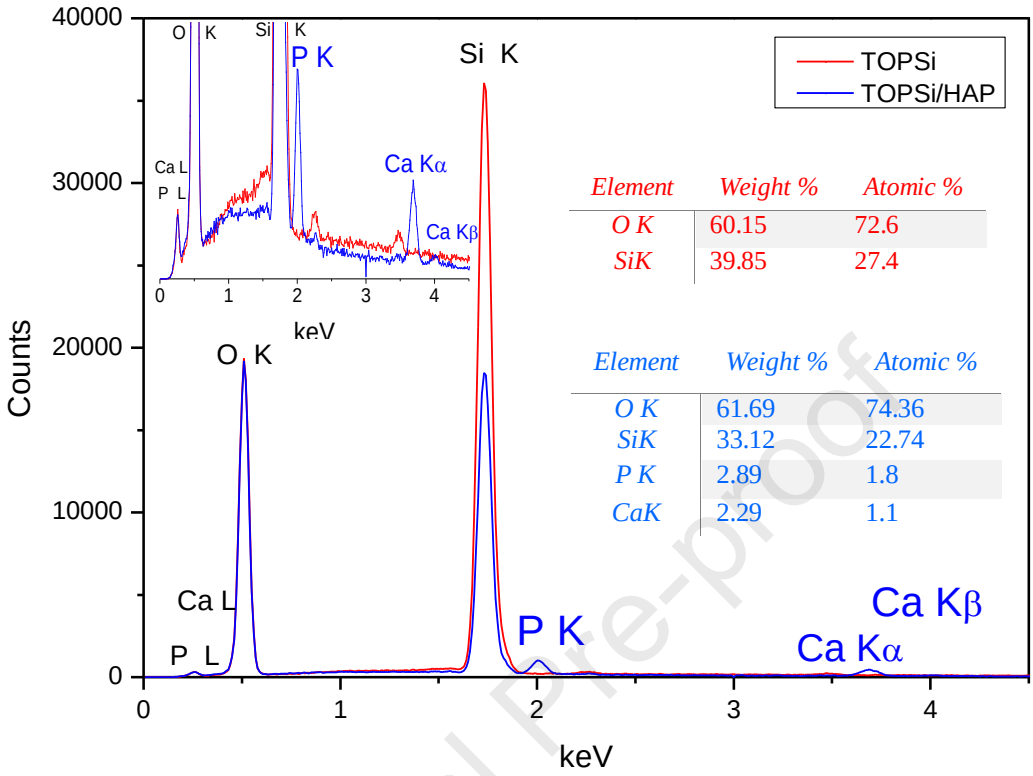


Fig. 4. EDS spectra of TOPSi, and TOPSi/HAP composite

According to the XRD pattern shown in Figure 5, two characteristic main peaks appeared around 2θ = 26° and 2θ = 32°, representing the HAP. The large peak at 2θ = 32° is attributed to many nanometer-sized and randomly orientated many crystal planes [13, 14]. The reason why the silicon peak is not visible is explained according to the ICDD standard for HA (JCPDS 09-432). According to this disclosure, the diffractive pattern of hydroxyapatite and the diffractive pattern of the silicon substrate might be similar as previously mentioned in ref. [15]. It is conclusively known that the broad peak at approximately 2θ = 21° in the XRD pattern indicates the presence of SiO_2 nanostructures [16]. Based on all these data, it is concluded that the crystal planes of HAP and SiO_2 nanostructures overlap and form broad peaks, as previously stated in the literature [13, 14]. The hexagonal $Ca(OH)_2$ phase was also present at approximately 2θ = 17.8° in the XRD pattern in the Fig. 5 [17].

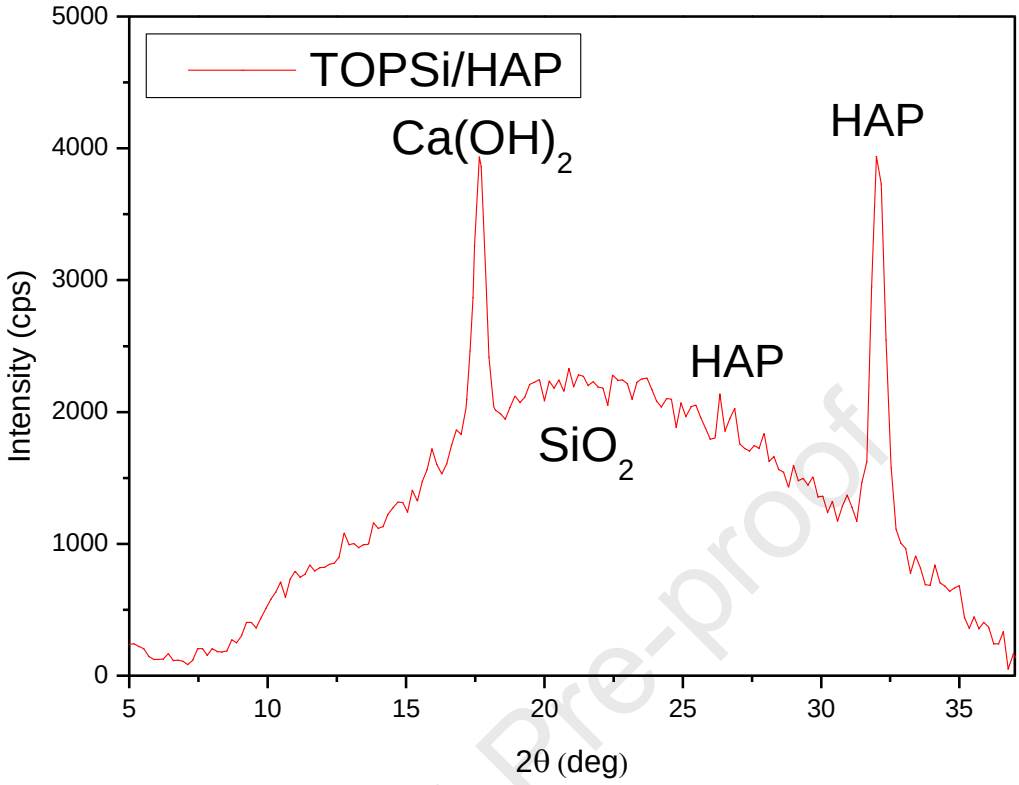
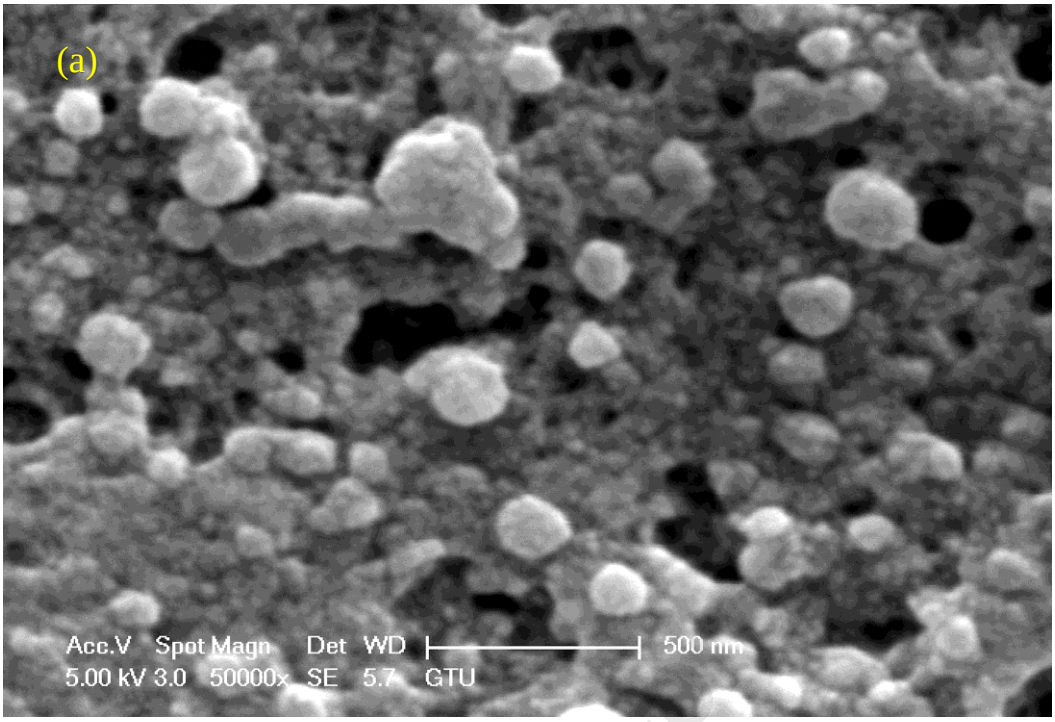


Fig. 5. XRD pattern of TOPSi/HAP

3.2. Characterization of SiCaPs

The SiCaPs were obtained by laser ablation of the TOPSi/HAP composite which was placed as a target in a pyrex beaker filled with distilled water, in a short pulse regime. Figure 6(a) shows SEM image of the SiCaPs. From the SEM image, it was clearly found out that the SiCaPs had a spherical shape. The EDS spectrum containing the table of the comparative proportion of the elements within the structure of the SiCaPs is shown in Figure 6(b). According to the EDS analysis results, SiCaPs are rich in Si, Ca, P, O. The Ca or P ratio can be adjusted according to the application purpose by changing the amount of HAP precursor solution to be coated on TOPSi. The Mg, Al, Na peaks are associated with the dropping procedure applied on the aluminum plate before the EDS analysis. The peak associated with Au is due to the Au coating procedure to ensure sufficient conductivity for the measurement of EDS. Ultra-pure SiCaPs were obtained without any chemical contamination.

Journal Pre-proof



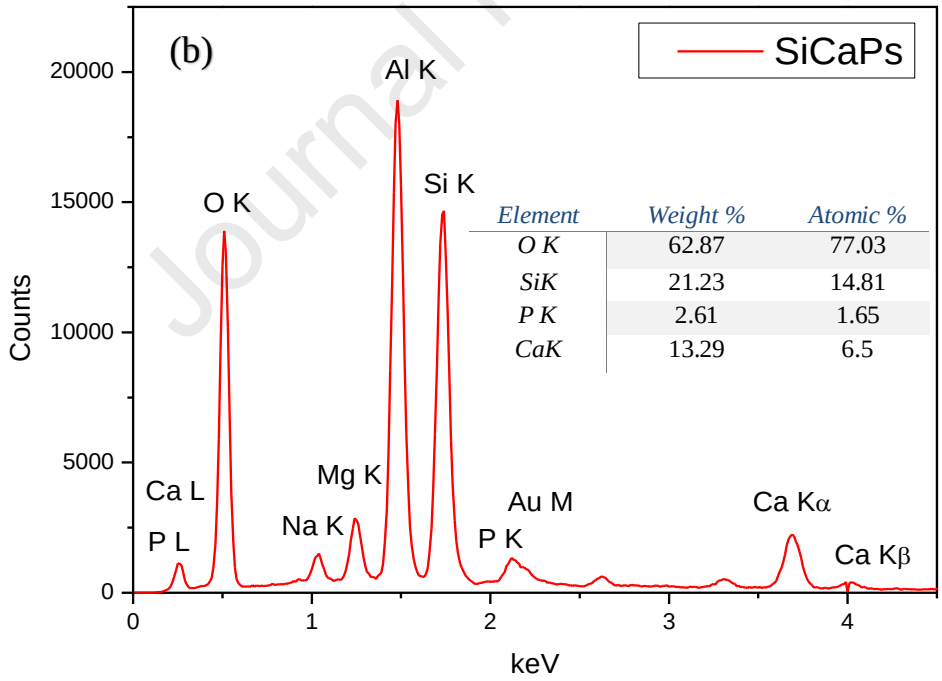


Fig. 6. SEM image **(a)** and EDS spectrum **(b)** of SiCaPs

FTIR spectroscopy ranging from 600-4000 cm^{-1} was used to investigate the bond vibration modes of SiCAPs as shown in Figure 7. Broadband absorption peak at 3320 cm^{-1} indicates the OH stretching

vibration of absorbed water [18]. FTIR peaks around 880, 1417 and 1455 cm^{-1} may indicate the carbonate ion in the HAP structure [19]. The FTIR peak appearing at 632 cm^{-1} is attributed to the asymmetric bending vibration of the P-O groups [19]. Between 1090-1010 cm^{-1}, the vibration peaks of the Si-O-Si and $(PO_4)^{3-}$ groups overlapped and two sharp peaks were observed. These two sharp peaks are attributed to the formation of tetramer and larger rings rather than cyclic siloxanes [12]. FTIR peaks around 803 cm^{-1} likely indicate Si-O-P and Si-O-Si vibrations [20]. The peak at 603 cm^{-1} is attributed to the formation of the CaP phase in the SiCaPs [19]. FTIR peaks between 1400-1500 cm^{-1} are asymmetric stretching vibrations of CO_3^{-2} [21]. FTIR peaks at 2973 and 2882 cm^{-1} can be interpreted as C-H organic residues [22].

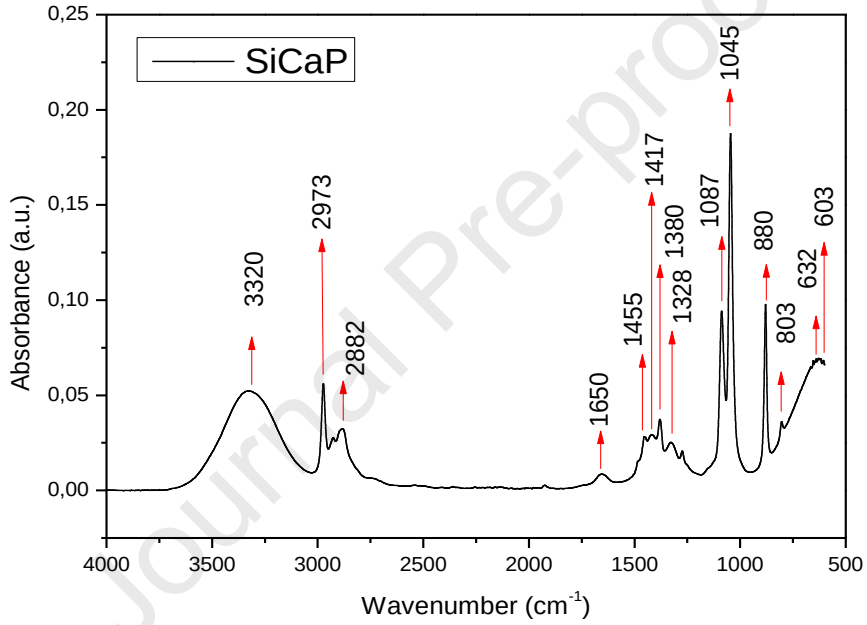


Fig. 7. FTIR spectrum of SiCaPs

DLS analysis results of the SiCaPs are shown in Figure 8(a). It was found that the hydrodynamic diameter of the particles ranged from 80 to 200 nm. The average hydrodynamic diameter was measured as 120 nm. Thus the particles were found to have a substantially homogeneous size distribution. According to the zeta potential results shown in Figure 8(b) and measured at 20 ° C, the zeta potential value of the particles was determined as -20 mV at Ph 4,5.

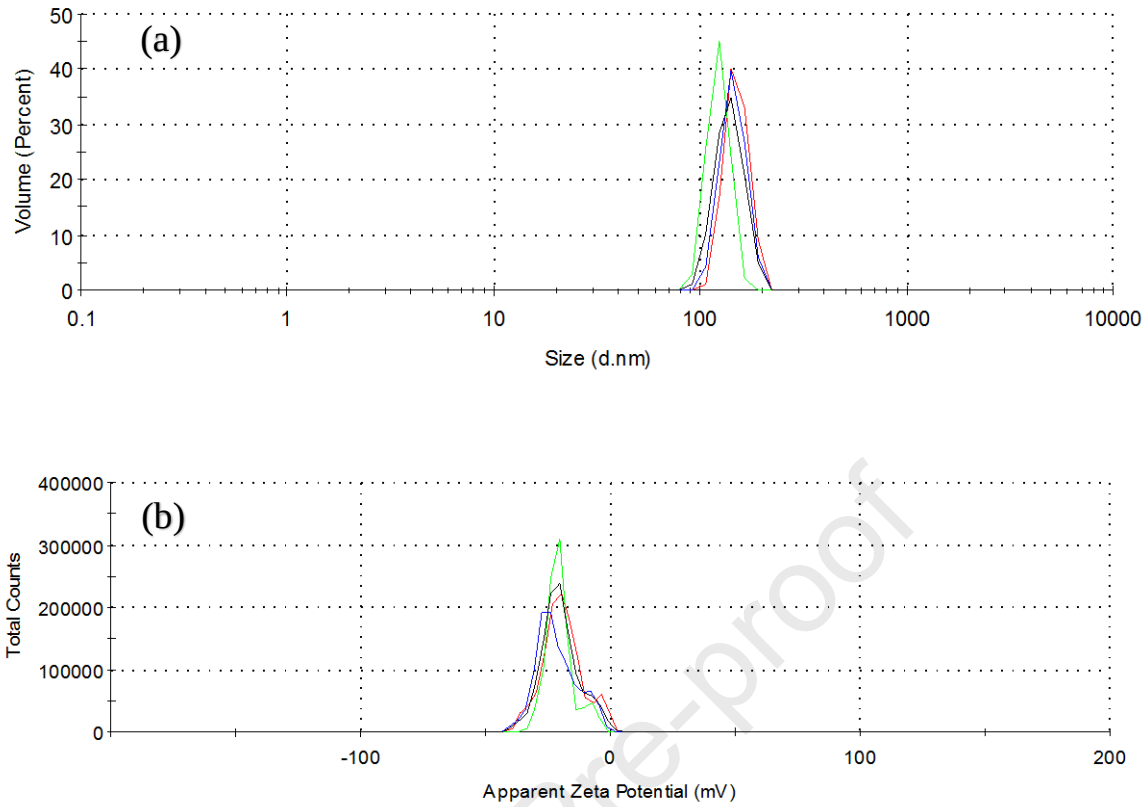


Fig. 8. DLS analysis **(a)** and Zeta Potential measurements **(b)** of SiCaPs

4. Conclusion

The plasma plume containing Ca, P, and Si, which was formed on TOPSi/HAP composite surface by virtue of laser ablation method, collapsed when it encountered the distilled water, and SiCaPs were formed. Ultra pure composite particles were synthesized with a unique approach without the use of harsh chemical procedures or any chemical contamination. Since SiCaPs synthesized by laser ablation method are ultra-pure, offer homogeneous size distribution, they will be a more preferred biomaterial in many biomedical applications in the future. Moreover, by changing some parameters of the synthesis conditions, SiCaPs having suitable properties for various biomedical applications can possibly be designed. In the future, various composite nanoparticles will be synthesized by laser ablation of porous silicon composites due to the fact that the sponge-like structure of porous silicon can absorb many materials and various composites can thus be formed.

CRediT Author Statement

Filiz KARAKUŞ BAŞAK: Conceptualization, Methodology, Formal analysis, Investigation, Data Curation, Writing - Original Draft, Writing - Review & Editing, Visualization, **Ersin KAYAHAN:** Validation, Formal analysis, Resources, Writing - Review & Editing, Supervision.

Acknowledgements

This study was supported by Kocaeli University Scientific Research Projects Coordination Unit [Project No. 2019/074 and 2016/068], Kocaeli University Laser Technologies Research and Application Center and KORDSA. The authors are grateful to Dr. Ahmet Y. ORAL of Gebze Technical University for his support in measuring DLS and Zeta Potential. We thank Dr. Necip YILDIZ for the English revision of this paper.

Compliance with ethical standards

No ethical clearance was required.

Conflict of interest

The authors declare no competing financial interests.

References

[1] Y. Jiang, Y. Han, J. Wang, F. Lv, Z. Yi, Q. Ke, H. Xu, Space-Oriented Nanofibrous Scaffold with Silicon-Doped Amorphous Calcium Phosphate Nanocoating for Diabetic Wound Healing, ACS Appl. Bio Mater. 2 (2019) 787–795. https://doi.org/10.1021/acsabm.8b00657.

[2] H.P. Rim, K.H. Min, H.J. Lee, S.Y. Jeong, S.C. Lee, PH-tunable calcium phosphate covered mesoporous silica nanocontainers for intracellular controlled release of guest drugs, Angew. Chemie - Int. Ed. 50 (2011) 8853–8857. https://doi.org/10.1002/anie.201101536.

[3] M. Mohammadi, S. Hesaraki, M. Hafezi-Ardakani, Investigation of biocompatible nanosized materials for development of strong calcium phosphate bone cement: Comparison of nano-titania, nano-silicon carbide and amorphous nano-silica, Ceram. Int. 40 (2014) 8377–8387. https://doi.org/10.1016/j.ceramint.2014.01.044.

[4] I. Variable, S. Tal, T. Garcia, (12) United States Patent (10) Patent No.: US 9,186,417 B2, 2 (2011). https://patents.google.com/patent/US9186417B2/en.

[5] Z. Wu, X. Wang, Z. Wang, C. Shao, X. Jin, L. Zhang, H. Pan, R. Tang, B. Fu, Self-Etch Adhesive as a Carrier for ACP Nanoprecursors to Deliver Biomimetic Remineralization, ACS Appl. Mater. Interfaces. 9 (2017) 17710–17717. https://doi.org/10.1021/acsami.7b01719.

[6] L.M. De Plano, S. Scibilia, M.G. Rizzo, S. Crea, D. Franco, A.M. Mezzasalma, S.P.P. Guglielmino, One-step production of phage–silicon nanoparticles by PLAL as fluorescent

nanoprobes for cell identification, Appl. Phys. A Mater. Sci. Process. 124 (2018) 0. https://doi.org/10.1007/s00339-018-1637-y.

[7] J. Xiao, P. Liu, C.X. Wang, G.W. Yang, External field-assisted laser ablation in liquid: An efficient strategy for nanocrystal synthesis and nanostructure assembly, Prog. Mater. Sci. 87 (2017) 140–220. https://doi.org/10.1016/j.pmatsci.2017.02.004.

[8] J. Hernandez-Montelongo, D. Gallach, N. Naveas, V. Torres-Costa, A. Climent-Font, J.P. García-Ruiz, M. Manso-Silvan, Calcium phosphate/porous silicon biocomposites prepared by cyclic deposition methods: Spin coating vs electrochemical activation, Mater. Sci. Eng. C. 34 (2014) 245–251. https://doi.org/10.1016/j.msec.2013.09.022.

[9] S.T. Kassim, H.A. Hadi, R.A. Ismail, Fabrication and characterization of high photosensitivity CuS/porous silicon heterojunction photodetector, Optik (Stuttg). 221 (2020) 165339. https://doi.org/10.1016/j.ijleo.2020.165339.

[10] R.A. Ismail, Fabrication and characterization of photodetector based on porous silicon, E-Journal Surf. Sci. Nanotechnol. 8 (2010) 388–391. https://doi.org/10.1380/ejssnt.2010.388.

[11] M. Prokopowicz, A. Szewczyk, A. Skwira, R. Sądej, G. Walker, Biphasic composite of calcium phosphate-based mesoporous silica as a novel bone drug delivery system, Drug Deliv. Transl. Res. 10 (2020) 455–470. https://doi.org/10.1007/s13346-019-00686-3.

[12] G. Socrates, Infrared and Raman characteristic group frequencies. Tables and charts, 2001. https://doi.org/10.1007/s00396-004-1164-6.

[13] L. Pramatarova, E. Pecheva, D. Dimova-Malinovska, R. Presker, M. Stutzmann, U. Schwarz, R. Kniep, A novel laser-liquid-solid interaction process for hydroxyapatite formation on porous silicon, 13th Int. Sch. Quantum Electron. Laser Phys. Appl. 5830 (2005) 110. https://doi.org/10.1117/12.618423.

[14] C. Shaoqiang, Z. Ziqiang, Z. Jianzhong, Z. Jian, S. Yanling, Y. Ke, W. Weiming, W. Xiaohua, F. Xiao, L. Laiqiang, S. Li, Hydroxyapatite coating on porous silicon substrate obtained by precipitation process, Appl. Surf. Sci. 230 (2004) 418–424. https://doi.org/10.1016/j.apsusc.2004.03.203.

[15] X.L. Tang, X.F. Xiao, R.F. Liu, Structural characterization of silicon-substituted hydroxyapatite synthesized by a hydrothermal method, Mater. Lett. 59 (2005) 3841–3846. https://doi.org/10.1016/j.matlet.2005.06.060.

[16] Munasir, Triwikantoro, M. Zainuri, Darminto, Synthesis of SiO_2 nanopowders containing quartz and cristobalite phases from silica sands, Mater. Sci. Pol. 33 (2015) 47–55. https://doi.org/10.1515/msp-2015-0008.

[17] A. Samanta, D.K. Chanda, P.S. Das, J. Ghosh, A.K. Mukhopadhyay, A. Dey, Synthesis of Nano Calcium Hydroxide in Aqueous Medium, J. Am. Ceram. Soc. 99 (2016) 787–795. https://doi.org/10.1111/jace.14023.

[18] Y. He, B. Zeng, S. Liang, M. Long, H. Xu, Synthesis of pH-Responsive Biodegradable Mesoporous Silica-Calcium Phosphate Hybrid Nanoparticles as a High Potential Drug Carrier, ACS Appl. Mater. Interfaces. 9 (2017) 44402–44409. https://doi.org/10.1021/acsami.7b16787.

[19] S. Mondal, A. Mondal, N. Mandal, B. Mondal, S.S. Mukhopadhyay, A. Dey, S. Singh, Physico-chemical characterization and biological response of Labeo rohita-derived hydroxyapatite scaffold, Bioprocess Biosyst. Eng. 37 (2014) 1233–1240. https://doi.org/10.1007/s00449-013-1095-z.

[20] M. Kamal, I.K. Battisha, M.A. Salem, A.M.S. El Nahrawy, Structural and thermal properties of monolithic silica-phosphate (SiO_2-P_2O_5) gel glasses prepared by sol-gel technique, J. Sol-Gel Sci. Technol. 58 (2011) 507–517. https://doi.org/10.1007/s10971-011-2420-0.

[21] M. López-Álvarez, E.L. Solla, P. González, J. Serra, B. León, A.P. Marques, R.L. Reis, Silicon-hydroxyapatite bioactive coatings (Si-HA) from diatomaceous earth and silica. Study of adhesion and proliferation of osteoblast-like cells, J. Mater. Sci. Mater. Med. 20 (2009) 1131–1136. https://doi.org/10.1007/s10856-008-3658-0.

[22] K. Mani Rahulan, G. Vinitha, S. Ganesan, R. Philip, P. Aruna, Synthesis and optical limiting studies of HAP and HAP@SiO2 core-shell nanoparticles, J. Mater. Sci. Mater. Electron. 23 (2012) 877–881. https://doi.org/10.1007/s10854-011-0510-y.

Journal Pre-proof

Journal Pre-proof

Declaration of interests

☒ The authors declare that they have no known competing financial interests or personal relationships that could have appeared to influence the work reported in this paper.

☐The authors declare the following financial interests/personal relationships which may be considered as potential competing interests:

Filiz KARAKUS BASAK Ersin KAYAHAN

Journal Pre-proof